CoMFA Modeling of Human Catechol *O*-Methyltransferase Enzyme Kinetics

Julius Sipilä* and Jyrki Taskinen

Division of Pharmaceutical Chemistry, Department of Pharmacy, University of Helsinki, P.O. Box 56, Viikinkaari 5E, 00014 University of Helsinki, Finland

Received August 29, 2003

Three-dimensional QSAR models with different charge calculation methods (MOPAC-AM1-ESP, MOPAC-AM1-Coulson and Gasteiger−Hückel) were developed for predicting all three enzyme kinetic parameters K_m, V_{max} and V_{max}/K_m for catecholic substrates of human soluble catechol *O*-methyltransferase (S-COMT). The empirical parameters of 45 substrates were correlated to the steric and electronic molecular fields of the substrates utilizing Comparative Molecular Field Analysis (CoMFA). Alignment rules for CoMFA were developed based on the catalytic mechanism and crystal structure of S-COMT, and the analysis was optimized using an all-space search technique. Leave-one-out and leave-n-out cross-validation (with 5 and 10 cross-validation groups) was carried out, and all developed models proved to be statistically significant with q^2 values up to 0.84. The models based on MOPAC charge calculations predicted the empirical values clearly better than the Gasteiger−Hückel method. The derived CoMFA coefficient contour maps of steric and electrostatic interactions correlated clearly with the S-COMT crystallographic structures.

INTRODUCTION

There is a growing need for molecular structure based modeling and prediction of absorption, distribution, metabolism, excretion and toxicity (ADMET) properties of new drug candidates in the early stages of drug discovery.[1,2] The ultimate goal is to achieve accurate and fast predictions of the metabolism routes and rates of new lead molecules to avoid possible drug-drug interactions and failures in the later stages of drug development. Catechol *O*-methyltransferase (COMT) is an important metabolizing enzyme that catalyzes the methylation of various catecholic substances such as catecholamines, catecholic estrogens and their metabolites as well as many therapeutic drugs. COMT is also interesting as a target molecule in the drug therapy of Parkinson's disease: inhibitors of this enzyme are used together with L-DOPA and DOPA decarboxylase (DDC) inhibitors.[3]

The biochemistry and molecular biology of COMT has recently been reviewed.[3] There are two forms of COMT coded by a single gene: the soluble, cytosolic form (S-COMT) and the membrane-bound form (MB-COMT) found in the rough endoplasmic reticulum.[4−7] COMT is expressed in almost all mammalian tissues, and the soluble form of the enzyme is predominant in all tissues except in the brain, where MB-COMT is expressed dominantly.[8−10] The tissue distribution and different selectivity of these two isoforms suggest that MB-COMT may be more involved in the regulation of catecholaminergic neurotransmission, while S-COMT plays an important role in the metabolism of endogenous and xenobiotic catechols in peripheric tissues.[11−14]

The X-ray crystallographic structure of S-COMT cocrystallized with AdoMet, magnesium-ion and 2,4-dinitrocatechol has been available since 1994.[15] Two more crystal structures of S-COMT with bound inhibitors have been reported recently.[16,17] The active site of COMT is a narrow hydrophobic pocket which tightly accommodates the aromatic ring of catecholic substrates (Figure 1). The catalytic mechanism of the enzyme involves a magnesium ion which is bound to the bottom of the hydrophobic pocket. The gatekeeper residues Trp38, Trp143 and Pro174 are responsible for the specificity and selectivity of the enzyme, and they also orient the reacting hydroxyl group in a favorable position for methyl transfer reaction.[3] In the published X-ray crystal structure the surface of the enzyme comes into close contact with the aromatic ring and the 3-nitro group of the bound substrate 3,5-dinitrocatechol. The groove that binds the aromatic ring is quite shallow allowing bulky substituents to be accommodated in the *meta* and *para* positions. It has been suggested that hydrophobic substituents are favored in the *para* position and polar substituents in the *meta* position.[18] This is supported by the in vivo observation that 3-*O*-methylated catecholamines are more common than their 4-*O*-methylated counterparts.

There are a few published two-dimensional QSAR studies of S-COMT inhibition.[19−21] In this study we successfully developed predictive three-dimensional QSAR models for the enzyme kinetic parameters K_m, V_{max} and V_{max}/K_m of the methylation reaction catalyzed by S-COMT. The aim of this paper is to present the development and validation of these QSAR models with a data set of 45 different catecholic substrates and to discuss the significance of the models.

MATERIAL AND METHODS

The Data Set. The evaluated data set consisted of 45 catecholic substrates of human S-COMT and corresponding enzyme kinetic parameters K_m, V_{max} and V_{max}/K_m (Table 1). The parameters were conversed to log K_m^{-1}, log V_{max} and log(V_{max}/K_m) for the analysis. The methods and results of the empirical determination of the enzyme kinetic parameters

* Corresponding author phone: +358 9 191 59171; fax: +358 9 191 59556; e-mail: julius.sipila@helsinki.fi.

10.1021/ci034189k CCC: $27.50
Published on Web 11/22/2003

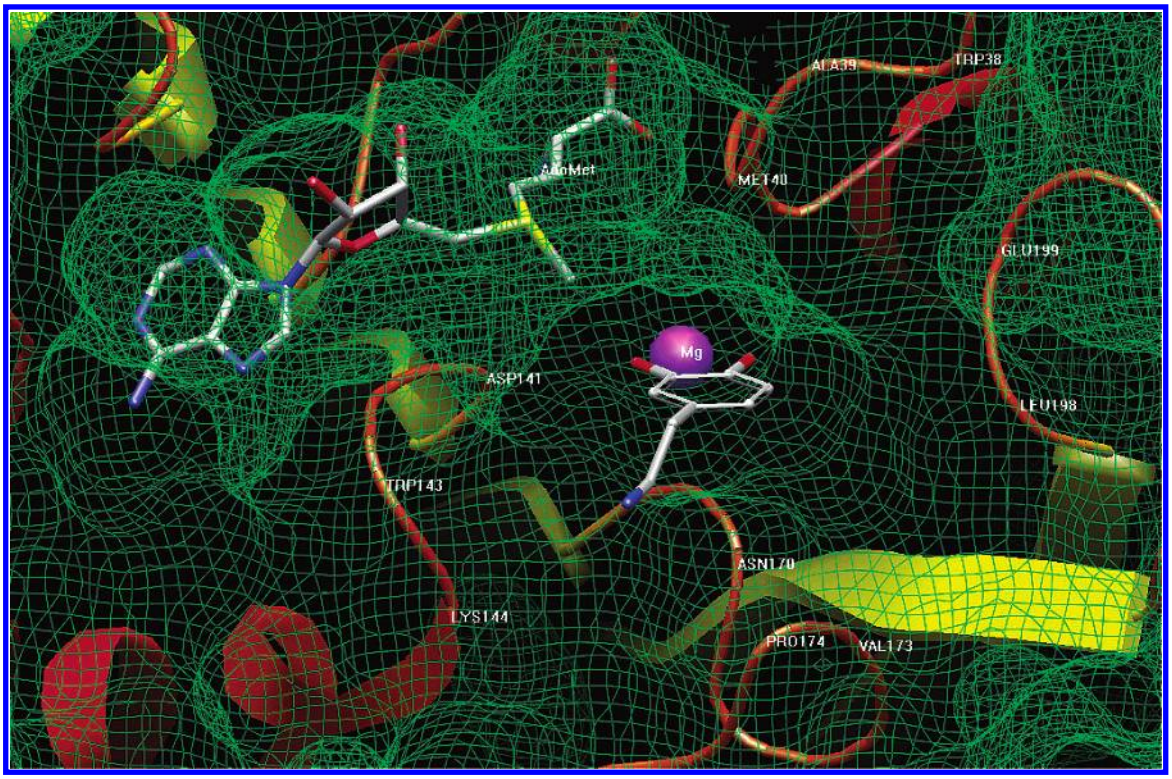

Figure 1. Dopamine and S-adenosyl-L-methionine (AdoMet) modeled in the active site of COMT crystal structure.[15] Dopamine is modeled for methylation in the favored *meta* position.

Table 1. Empirical and Calculated Parameters log K_m^{-1}, log V_{max} and log(V_{max}/K_m) of All Compounds in the Data Set from the Models II, V and VIII Where Semiempirical ESP Charges Were Used

	empirical log K_m^{-1}	log K_m^{-1} model II	empirical log V_{max}	log V_{max} model V	empirical log (V_{max}/K_m)	log(V_{max}/K_m) model VII
2,3-dihydroxybenzoic acid	3.42[a]	4.53				
2,3-dihydroxynaphthalene	5.82	5.28	1.48	1.54	1.31	1.01
2-hydroxyestradiol	5.43	4.97	1.66	2.02	1.1	0.89
3,4-dihydroxyacetophenone	5.85	6.06	0.99	0.87	0.85	0.99
3,4-dihydroxybenzoic acid	4.70	4.89	1.64	1.49	0.34	0.54
3,4-dihydroxymandelic acid	3.88	4.31	1.64	1.51	−0.48	−0.3
3,4-dihydroxyphenylacetic acid	4.14	4.14	1.58	1.53	−0.26	−0.21
3,4-dihydroxyphenylglycol	4.33	4.42	1.57	1.33	−0.1	−0.2
3-fluorocatechol	5.11	5.10	1.49	1.24	0.6	0.43
3-methoxy-5-bromocatechol	5.59	5.43	1.24	1.32	0.84	0.94
3-methoxycatechol	4.61	4.23	1.60	1.71	0.21	0.4
3-nitrocatechol	7.70[a]	7.21	−0.82	−0.53	0.88	0.91
4-chlorocatechol	4.93	5.54	1.56	1.25	0.49	0.69
4-hydroxyestradiol	4.91	4.83	1.50	1.63	0.41	0.44
4-isopropylcatechol	4.58	4.59	1.64	1.57	0.22	0.06
4-methoxy-5-*tert*-butylcatechol	4.73	4.32	1.52	1.64	0.25	−0.004
4-methylcatechol	4.54	5.06	1.68	1.50	0.22	0.55
4-nitrocatechol	6.92[a]	6.96	0.19	0.20	1.11	1.06
4-*tert*-butylcatechol	4.50	4.47	1.62	1.64	0.12	−0.08
5-hydroxydopamine	4.21	4.32	1.67	1.67	−0.12	0.13
6,7-dihydroxycoumarin	6.52[a]	6.85	0.52	0.38	1.04	0.96
6-hydroxydopamine	3.61	3.81	1.40	1.53	0.98	0.52
adrenaline	3.88	3.81	1.64	1.59	−0.48	−0.57
amedopa	2.75	2.69	1.38	1.31	−1.92	−1.99
apomorphine	3.62[a]	3.45				
benserazide	4.30	4.11	1.62	1.63	−0.08	−0.23
caffeic acid	5.49	5.73	1.62	1.50	1.11	1.13
carbidopa	3.22	3.00	1.16	1.26	−1.62	−1.56
catechol	4.30	4.14	1.69	1.82	−0.01	0.09
dihydrexidine	4.60	4.47	1.31	1.12	−0.08	−0.31
dobutamine	4.64	4.58	1.56	1.57	0.18	−0.02
dopamine	3.73	3.58	1.56	1.66	−0.72	−0.81
entacapone	9.50[a]	9.38		−1.12		
ethyl-3,4-dihydroxybenzoate	6.18[a]	6.18	1.03	1.02	1.21	1.19
hydrocaffeic acid	4.60	4.54	1.64	1.78	0.23	0.31
isoprenaline	3.84	3.82	1.46	1.68	−0.7	−0.55

Table 1 (Continued)

	empirical log K_m^{-1}	log K_m^{-1} model II	empirical log V_{max}	log V_{max} model V	empirical log (V_{max}/K_m)	log(V_{max}/K_m) model VII
levodopa	3.25	3.23	1.47	1.39	−1.28	−1.26
levodopa metester	4.29	4.33	1.65	1.63	−0.06	−0.03
methylgallate	6.00	6.13	1.07	1.10	1.07	1.13
noradrenaline	3.59	3.66	1.52	1.56	−0.89	−0.25
pyrogallol	4.98	4.39	1.73	1.63	0.71	0.5
salsilinol	4.53	4.86	1.46	1.46	−0.01	0.19
skf38393	4.14	4.43	1.19	1.12	−0.68	−0.73
tetrachlorocatechol	7.52[a]	7.12	−0.21	0.17	1.33	1.35
tolcapone	9.60[a]	9.61		−0.97		

[a] Inhibition constant K_i was used for K_m.

Table 2. Statistics of CoMFA Models I−VII[a]

model	charge	*N*	q^2	S_{PRESS}	*C*	*F*	SE	r^2
I log (1/K_m)	Gasteiger−Hückel	45	0.59	0.99	4	82	0.51	0.89
II log (1/K_m)	ESP (MOPAC)	45	0.77	0.76	5	163	0.34	0.95
III[b] log (1/K_m)	ESP (MOPAC)	44	0.84	0.63	5	293	0.25	0.98
IV[c] log V_{max}	Gasteiger−Hückel	43	0.50	0.54	5	54	0.27	0.88
V[c] log V_{max}	ESP (MOPAC)	43	0.74	0.39	5	160	0.16	0.96
VI[d] log (V_{max}/K_m)	Gasteiger−Hückel	41	0.43	0.64	5	118	0.20	0.94
VII[d] log (V_{max}/K_m)	ESP (MOPAC)	41	0.57	0.56	5	106	0.21	0.94

[a] *N* = number of training set compounds, q^2 = cross-validated (leave-one-out) predictive r^2 of the model, S_{PRESS} = standard error of prediction, *C* = optimum number of PLS components, *F* = *F* value of the model, SE = standard error of the model, r^2 = conventional r^2 of the model. [b] 2,3-Dihydroxybenzoic acid was dropped out from model III. [c] Apomorphine and 2,3-dihydroxybenzoic acid were not included in models IV and V. [d] Apomorphine, 2,3-dihydroxybenzoic acid, entacapone and tolcapone were not included in models VI and VII.

used in this study have been published previously.[11,21] The K_m value for nine compounds (4-nitrocatechol, 3-nitrocatechol, tetrachlorocatechol, 6,7-dihydroxycoumarin, ethyl 3,4-dihydroxybenzoate, apomorphine, 2,3-dihydroxybenzoic acid, entacapone and tolcapone) was determined as the K_i value for competitive inhibition. Four substrates in the data set (apomorphine, 2,3-dihydroxybenzoic acid, entacapone and tolcapone) for which the V_{max} value could not be determined were omitted from the initial models where log V_{max} or log(V_{max}/K_m) was used as the dependent variable. However, as methylated metabolites of entacapone and tolcapone are known to exist in vivo,[22,23] we also built a separate model with an approximated V_{max} value that is in the range of the detection limit of the quantification method (log $V_{max} = -1$).

Computational Methods. All computations were performed on SGI Octane workstations using molecular modeling software packages SPARTAN (version 5.0, Wavefunction Inc., Irvine, CA) and SYBYL (version 6.8, Tripos Inc., St. Louis, MO) for building minimum energy conformations of substrate molecules and CoMFA calculations, respectively. The pK_a values of the substrates were estimated with the ACD/LogD program (version 4.0, Advanced Chemistry Development Inc., Toronto, ON, Canada). Substrate molecular conformations were optimized to the semiempirical AM1 level. Gasteiger−Hückel, electrostatic potential fitted (ESP) and Coulson atomic partial charges were calculated using SYBYL and the quantum chemistry extension MOPAC (Quantum Chemistry Program Exchange, Indiana University, IN). To automate the calculations several Sybyl Programming Language (SPL) scripts were developed.

Table 3. Leave-n-Out Cross-Validation of ESP Fitted Charge Models[a]

model	charge	*N*	*N*	mean	SD
II	ESP (MOPAC)	45	5	0.74	0.052
log(1/Km)			10	0.75	0.034
III[b]	ESP (MOPAC)	44	5	0.82	0.030
log (1/Km)			10	0.84	0.017
V[c]	ESP (MOPAC)	43	5	0.69	0.07
log V_{max}			10	0.72	0.04
VII[d]	ESP (MOPAC)	41	5	0.52	0.07
log (V_{max}/K_m)			10	0.55	0.04

[a] *N* = number of cross-validation groups, mean = mean cross-validated q^2, SD = standard deviation of q^2 values. All runs were repeated 100 times. [b] 2,3-Dihydroxybenzoic acid was dropped out from model III. [c] Apomorphine and 2,3-dihydroxybenzoic acid were not included in model V. [d] Apomorphine, 2,3-dihydroxybenzoic acid, entacapone and tolcapone were not included in model VII.

CoMFA Alignment Rules. The substrate molecules were aligned based on existing knowledge of S-COMT crystal structure and substrate binding. Studying the published X-ray structure[15] revealed that the tight substrate binding pocket of S-COMT can accommodate a relatively small substituent adjacent to the reacting hydroxyl. It has been shown that catecholamine methylation by S-COMT prefers the *meta* position.[11,24] Hydrophobic substituents in *para* position generally improve substrate binding to the enzyme.[19,20] Based on these pieces of information the following alignment rules were derived: (1) catecholic oxygen atoms and aromatic carbons of all substrates were superimposed using least-squares fit (FIT ATOMS −procedure in SYBYL); (2) all

substituents in position 3 were aligned to the same side; (3) polar substituents were aligned in *meta* position; and (4) hydrophobic substituents were aligned in *para* position.

CoMFA Parameters. Tripos standard steric and electrostatic fields were used in all CoMFA calculations. Standard parameters were used for all fields: steric and electrostatic potentials were calculated with a +1 charged sp^3 carbon probe, smooth transition and a cutoff value of 30 kcal/mol. The CoMFA grid spacing was at 2 Å in all calculations, as lowering the grid spacing from this frequently used value did not improve the correlations in the initial studies. Michaelis constant values conversed to $\log(1/K_m)$ were used as a dependent variable column in models I−III. Log V_{max} and $\log(V_{max}/K_m)$ were used as dependent variables in models IV−V and VI−VII, respectively. To optimize the orientation of the substrates to the CoMFA grid an all space search technique described elsewhere in detail[25] was used. In all space search procedure the aligned substrate molecules are systematically rotated and translated in three-dimensional space to obtain the most consistent model. In this analysis the rotational space was evaluated rotating the substrates around x-, y- and z-axes by an increment of 30 degrees. Translational space was analyzed translating the substrates 2 Å in each direction by an increment of 0.2 Å. In these orientation/translation analyses the column filter was set at 1 kcal/mol, and the models with highest cross-validated q^2 (leave-one-out) values were selected for further validation.

PLS (Partial Least Squares) Model Validation. After all space search optimization the selected models were validated using leave-one-out and leave-n-out cross-validation procedures. In leave-one-out cross-validation the PLS model is rebuilt omitting each compound of the data set one at a time. This model is used to predict the activity of the omitted compound, and when the procedure is repeated through the whole data set cross-validated r^2 (q^2) values and standard error of predictions can be calculated. In leave-n-out cross-validation n compounds are omitted from the analysis each time when rebuilding the PLS models. Leave-n-out cross-validation was carried out for all PLS models using 5 and 10 randomly selected cross-validation groups. This was repeated 100 times, and mean q^2 values were reported. All validation runs were computed using no column filtering and with CoMFA standard preanalysis scaling.

Final PLS Model. After validation runs a final CoMFA analysis with an optimum number of PLS components and no validation was performed to obtain graphical contour coefficient maps and conventional r^2 and standard error values.

RESULTS

CoMFA models with three different charge calculation methods were built for predicting the K_m, V_{max} and V_{max}/K_m values of S-COMT substrates. The MOPAC charge calculation methods (ESP and Coulson charges) performed clearly better than Gasteiger−Hückel method in all cases. Data from the Coulson calculations is not shown, because there was no significant difference between the ESP and Coulson charge calculation methods (Table 1).

None of the models could predict the K_m value of 2,3-dihydroxybenzoic acid accurately, and a separate model was built without this outlier in the data set (Model III).

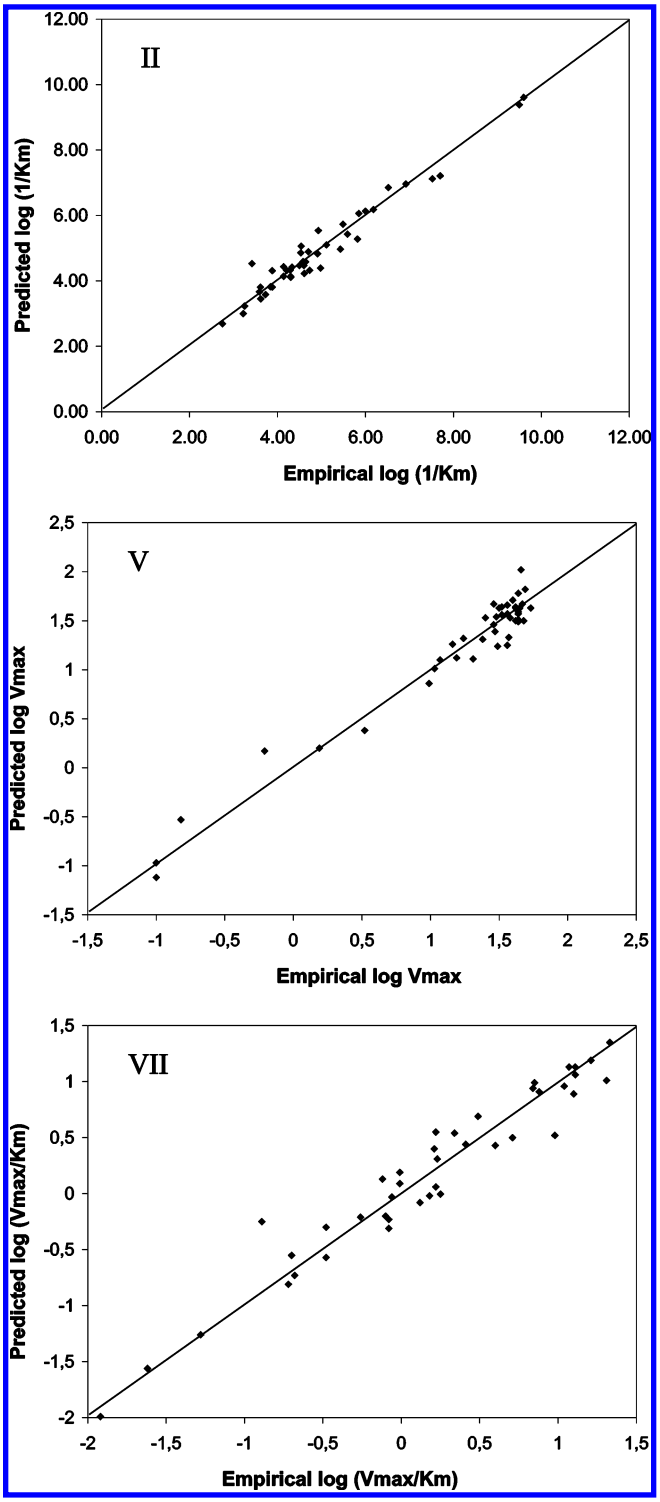

Figure 2. Plots of fitted vs empirical of ESP charge models II ($\log(1/K_m)$), V ($\log V_{max}$) and VII ($\log(V_{max}/K_m)$).

In the initial V_{max} model we omitted all four compounds (apomorphine, 2,3-dihydroxybenzoic acid, entacapone and tolcapone) for which the V_{max} value could not be determined. This model failed in the leave-one-out cross-validation ($q^2 = 0.24$ with five PLS components) although there was a clear correlation (conventional $R^2 = 0.94$). To create a predictive V_{max} model we used approximated V_{max} values ($\log V_{max} = -1$) for entacapone and tolcapone which are known to be (poor) substrates of COMT.[22,23] With these low-reactivity substrates included the final V_{max} model (model

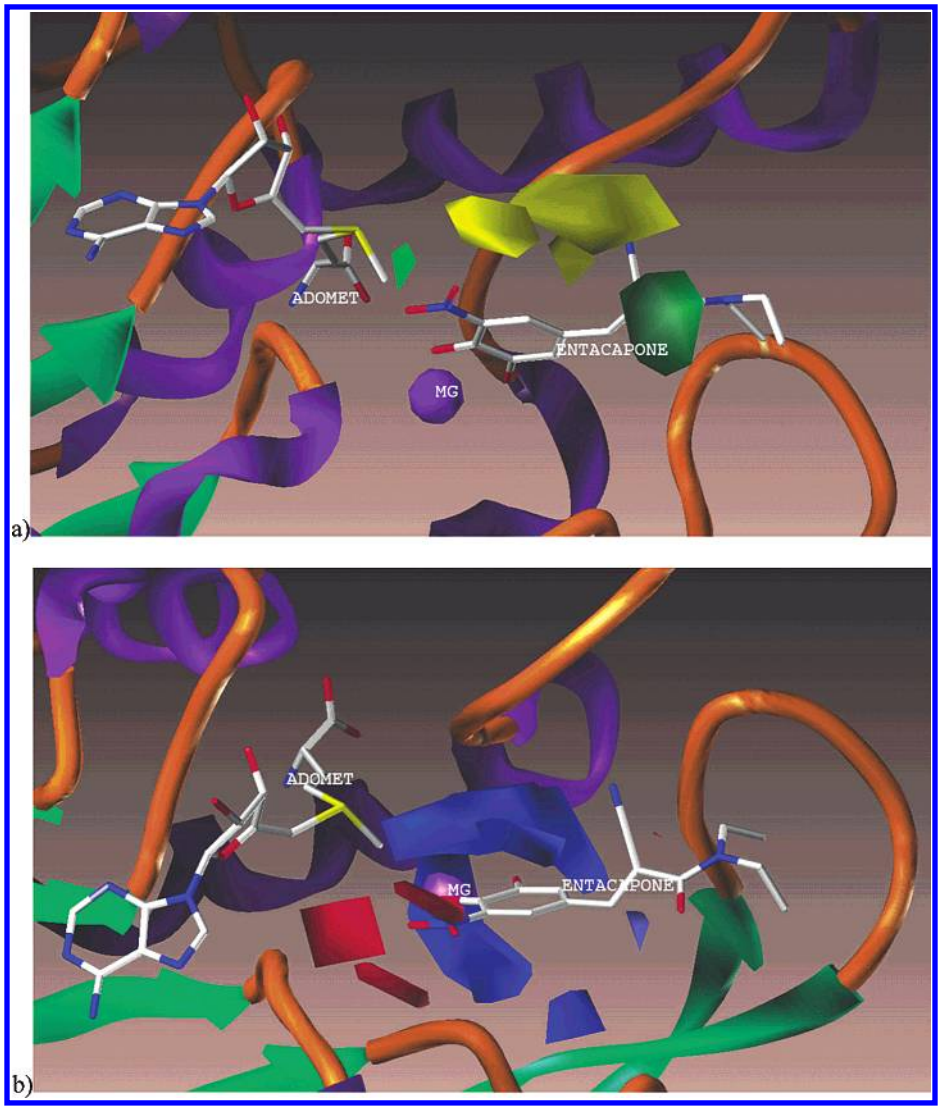

Figure 3. (a) Coefficient contour maps of steric interactions from model II (dependent variable = $\log(1/K_m)$) at the active site of s-COMT with the inhibitor entacapone. Green and yellow colors denote favorable and unfavorable regions for bulky substituents, respectively. (b) Coefficient contour maps of electronic interactions from model II at the active site of s-COMT with the inhibitor entacapone. The positive charge is favored near blue regions and the negative charge near red-colored regions.

V) proved to be robust also in the leave-one-out cross-validation runs ($q^2 = 0.74$ with five PLS components).

All final CoMFA models were robust in leave-n-out and leave-one-out cross-validation (Tables 2 and 3). The leave-one-out cross-validated q^2-values ranging from 0.43 to 0.84 give a good measure of the statistical significance of the models.

Studying the residual plots of the models (Figure 2) revealed some compounds for which the difference between fitted and actual K_m values was larger than one logarithmic unit. The most obvious outlier was 2,3-dihydroxybenzoic acid, for which the cross-validated prediction error was greater than 2 logarithmic units in all three models. Also the difference between the fitted and actual K_m-values of 2,3-dihydroxybenzoic acid was considerably high in all final models where it was included. The exclusion of this one outlier in the data set improved the correlations significantly (model III, Table 2).

CoMFA coefficient contour maps of regions of steric and electronic interactions from models II and V are visualized in Figures 3 and 4.

We studied also the correlation between the charge of the reacting hydrogen calculated with different methods and the estimated pK_a value. The MOPAC charges (ESP and Coulson) correlated clearly with the pK_a values ($R^2 = 0.54$ and $R^2 = 0.48$, respectively). There was no such correlation with the Gasteiger−Hückel charge calculation method ($R^2 = 0.01$).

DISCUSSION

CoMFA methodology has been successfully applied to various QSAR-analysis problems and characterizations of structural features that affect ligand binding to a given protein. We were able to develop statistically robust CoMFA models of human soluble COMT which can be used to predict all three enzyme kinetic parameters K_m, V_{max} and V_{max}/K_m for substituted catechol substrates of this important metabolizing enzyme.

In any CoMFA the most critical and demanding step is to find the active conformations of the substrates or ligands. The next phase, as crucial as the first step, is the mutual

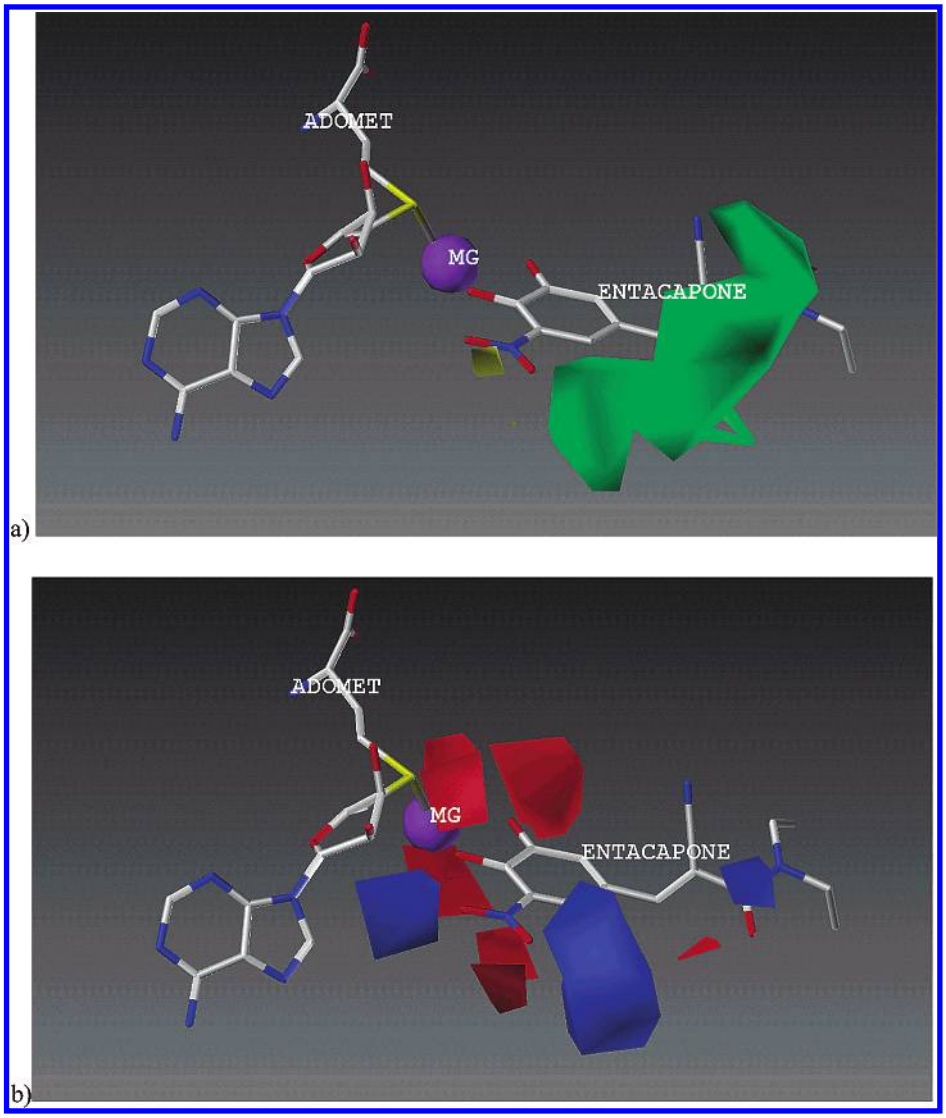

Figure 4. (a) Coefficient contour maps of steric interactions from model V (dependent variable = log V_{max}) with the inhibitor entacapone, magnesium-ion and the cosubstrate AdoMet. Green and yellow colors denote favorable and unfavorable regions for bulky substituents, respectively. (b) Coefficient contour maps of electronic interactions from model V at the active site of s-COMT with the inhibitor entacapone. The positive charge is favored near blue regions and the negative charge near red-colored regions. The protein structure has been omitted from this picture for reasons of clarity.

alignment of the substrates. Catechol *O*-methyltransferase is a highly specific enzyme for the catecholic group. The published X-ray structures of this enzyme support the assumption that the binding mode of the catecholic moiety is basically the same for all substrates of COMT which makes the alignment procedure quite straightforward. The active conformations of the substituents in the *meta* and *para* positions are more doubtful. It is reasonable to believe that interactions with the residues forming the outer surface of the binding pocket affect the conformation of the substrate side chains.

Docking methods have been successfully implemented in 3D QSAR studies for defining active conformers and alignments.[26−31] In the case of COMT we used a simple superposition procedure for minimum energy conformations of the substrates. The alignment was based on the existing knowledge of the structure of the substrate binding site and favorable methylation positions of substrates. Substituents in *meta* and *para* positions point out of the surface of the enzyme and they most probably have several possible active conformational states. Therefore using minimum energy conformations for building the model is well-grounded, especially given the good statistical results of the finished models.

There were some compounds for which the prediction of affinity was not accurate. The most obvious outlier, 2,3-dihydroxybenzoic acid, is a unique compound in this data set. One of the negatively charged oxygen atoms of this compound is close to the methyl group of AdoMet and to the catalytic base Lys 144 when fitted to the crystal structure of COMT. This electrostatic effect may interfere with the reaction mechanism as suggested by Lautala et al.[21] in a way the current models cannot account for.

There were four compounds in the data set (apomorphine, 2,3-dihydroxybenzoic acid, entacapone and tolcapone) for which the V_{max} value could not be determined because of low reactivity. Even so, two of these compounds are known substrates of COMT (entacapone and tolcapone) and leaving them out of the analysis would have resulted in loss of information. We tried two different estimated log V_{max} values in range of the detection limit (log $V_{max} = -1$ and -2) for these compounds. The V_{max} predicting models presented in

this paper (models IV and V) are based on the log V_{max} value of −1 for these low reactivity substrates as the statistics of the finished models were slightly better with this estimate.

Three CoMFA models with different atomic partial charge calculation methods were built and evaluated. The quantum mechanical semiempirical methods (AM1-ESP and AM1-Coulson) performed clearly better than Gasteiger−Hückel method in predicting the activity of the data set compounds. This is probably due to the fact that electron-withdrawing effects of the substituents attached to the catecholic ring are better described with the quantum mechanical methods. There is a clear correlation between ESP and Coulson charges of the reacting hydrogen and the estimated pK_a value of the substrate, which is not the case with the Gasteiger−Hückel method. It has been suggested that these electronic effects are the most important factor lowering K_m values of COMT inhibitors and substrates.[19−21] The statistically best models were achieved using charges fitted to the electrostatic potential.

The derived CoMFA region maps of K_m predicting (models I−III) correlated well with the COMT crystal structure. A clear region of K_m lowering interaction with bulk is visible *para* to the reacting hydroxyl group in the plane of the substrate's aromatic ring. Above the plane of the ring (Figure 3a) there is a region where steric bulk increases the K_m value. These regions are consistent with the possible hydrophobic and repelling interactions with gatekeeper residues Trp38 and Pro174. There is also a small region where steric bulk lowers the K_m value in the plane of the aromatic ring at the *ortho* position of the reacting hydroxyl. In this position there is some volume capable of accommodating a small substituent (for example a nitro group) also in the published crystal structure of the enzyme.

Existing knowledge of S-COMT structure and catalytic mechanism facilitates the interpretation of electrostatic CoMFA region maps. The electrostatic effects are probably mainly caused by the influence on the polarization of the reacting hydroxyl group rather than by direct interactions with charged groups of the enzyme. The CoMFA method itself with the parametrization used in this study cannot differentiate between these two types of electronic interaction. The electrostatic CoMFA maps reveal an extensive region where more positive charge lowers the K_m value around the catecholic hydroxyls. This region is consistent with the fact that the polarization state of the hydroxyl group has a major effect on the binding of the substrate. There are also regions where negative charge improves affinity in the *ortho* position of the reacting hydroxyl. It has been previously shown that small electron-withdrawing substituents in this position enhance the affinity of the substrate.[19,20]

The CoMFA region maps of V_{max} predicting models showed some inverse regions of interaction when compared with the K_m predicting models, especially when electronic effects are considered. This result could be interpreted as meaning that electronic effects which lower the K_m value also limit the maximum rate of the methylation reaction at the same time.

The QSAR models presented in this paper can be used to generate fast molecular structure-based predictions of all three enzyme kinetic parameters K_m, V_{max} and V_{max}/K_m of substituted catechols methylated by S-COMT. The estimated errors of prediction are relatively small, and the accuracy of the models is adequate to various purposes where rough estimates of the parameters in question are needed and empirical determinations are either too costly or time-consuming. Anyway, it should be noted that these in silico predictions are rather suggestive, and their usage is limited to compounds structurally related to the substrates in the data set.

ACKNOWLEDGMENT

This work was supported by the Finnish Graduate School in Pharmaceutical Research (Universities of Helsinki and Kuopio). We thank Prof. Luhua Lai (Institute of Physical Chemistry, Peking University, P.R. China) for providing the scripts for the CoMFA all space search calculations.

REFERENCES AND NOTES

(1) van de Waterbeemd, H.; Gifford, E. ADMET in silico modelling: Towards prediction paradise? *Nature Rev. Drug Discovery* **2003**, *2*, 192−204.
(2) Butina, D.; Segall, M. D.; Frankcombe, K. Predicting ADME properties in silico: methods and models. *Drug Discovery Today* **2002**, *7*, 83−88.
(3) Mannisto, P. T.; Kaakkola, S. Catechol-O-methyltransferase (COMT): biochemistry, molecular biology, pharmacology, and clinical efficacy of the new selective COMT inhibitors. *Pharmacol. Rev.* **1999**, *51*, 593−628.
(4) Tilgmann, C.; Kalkkinen, N. Purification and partial sequence analysis of the soluble catechol-O-methyltransferase from human placenta: comparison to the rat liver enzyme. *Biochemical Biophysical Res. Commun.* **1991**, *174*, 995−1002.
(5) Lundstrom, K.; Salminen, M.; Jalanko, A.; Savolainen, R.; Ulmanen, I. Cloning and characterization of human placental catechol-O-methyltransferase cDNA. *DNA Cell Biology* **1991**, *10*, 181−189.
(6) Bertocci, B.; Miggiano, V.; Da Prada, M.; Dembic, Z.; Lahm, H. W.; Malherbe, P. Human catechol-O-methyltransferase: cloning and expression of the membrane-associated form. *Proc. Natl. Acad. Sci. U.S.A.* **1991**, *88*, 1416−1420.
(7) Salminen, M.; Lundstrom, K.; Tilgmann, C.; Savolainen, R.; Kalkkinen, N.; Ulmanen, I. Molecular cloning and characterization of rat liver catechol-O-methyltransferase. *Gene* **1990**, *93*, 241−247.
(8) Karhunen, T.; Tilgmann, C.; Ulmanen, I.; Julkunen, I.; Panula, P. Distribution of catechol-O-methyltransferase enzyme in rat tissues. *J. Histochemistry Cytochemistry* **1994**, *42*, 1079−1090.
(9) Tenhunen, J.; Salminen, M.; Jalanko, A.; Ukkonen, S.; Ulmanen, I. Structure of the rat catechol-O-methyltransferase gene: separate promoters are used to produce mRNAs for soluble and membrane-bound forms of the enzyme. *DNA Cell Biology* **1993**, *12*, 253−263.
(10) Tenhunen, J.; Salminen, M.; Lundstrom, K.; Kiviluoto, T.; Savolainen, R.; Ulmanen, I. Genomic organization of the human catechol O-methyltransferase gene and its expression from two distinct promoters. *Eur. J. Biochemistry* **1994**, *33*, 1049−1059.
(11) Lotta, T.; Vidgren, J.; Tilgmann, C.; Ulmanen, I.; Melen, K.; Julkunen, I.; Taskinen, J. Kinetics of Human Soluble and Membrane-Bound Catechol O-Methyltransferase − a Revised Mechanism and Description of the Thermolabile Variant of the Enzyme. *Biochemistry* **1995**, *34*, 4202−4210.
(12) Mannisto, P. T.; Ulmanen, I.; Lundstrom, K.; Taskinen, J.; Tenhunen, J.; Tilgmann, C.; Kaakkola, S. K. Characteristics of catechol O-methyltransferase (COMT) and properties of selective COMT inhibitors. *Prog. Drug Res.* **1992**, *39*, 291−350.
(13) Roth, J. A. Membrane-bound catechol-O-methyltransferase: a reevaluation of its role in the O-methylation of the catecholamine neurotransmitters. *Rev. Physiol. Biochemistry Pharmacol.* **1992**, *120*, 1−29.
(14) Bonifati, V.; Meco, G. New, selective catechol-O-methyltransferase inhibitors as therapeutic agents in Parkinson's disease. *Pharmacol. Therapeutics* **1999**, *81*, 1−36.
(15) Vidgren, J.; Svensson, L. A.; Liljas, A. Crystal-Structure of Catechol O-Methyltransferase. *Nature* **1994**, *368*, 354−358.
(16) Lerner, C.; Ruf, A.; Gramlich, V.; Masjost, B.; Zurcher, G.; Jakob-Roetne, R.; Borroni, E.; Diederich, F. X-ray crystal structure of a bisubstrate inhibitor bound to the enzyme catechol-O-methyltransferase: a dramatic effect of inhibitor preorganization on binding affinity. *Angew. Chem., Int. Ed.* **2001**, *40*, 4040−4042.
(17) Bonifacio, M. J.; Archer, M.; Rodrigues, M. L.; Matias, P. M.; Learmonth, D. A.; Carrondo, M. A.; Soares-Da-Silva, P. Kinetics and

crystal structure of catechol-O-methyltransferase complex with co-substrate and a novel inhibitor with potential therapeutic application. *Mol. Pharmacol.* **2002**, *62*, 795−805.
(18) Lan, E. Y.; Bruice, T. C. Importance of correlated motions in forming highly reactive near attack conformations in catechol O-methyltransferase. *J. Am. Chem. Soc.* **1998**, *120*, 12387−12394.
(19) Taskinen, J.; Vidgren, J.; Ovaska, M.; Backstrom, R.; Pippuri, A.; Nissinen, E. Qsar and Binding Model for Inhibition of Rat-Liver Catechol-O-Methyl-Transferase by 1,5-Substituted-3,4-Dihydroxybenzenes. *Quant. Struct.−Act. Relat.* **1989**, *8*, 210−213.
(20) Lotta, T.; Taskinen, J.; Backstrom, R.; Nissinen, E. Pls Modeling of Structureactivity-Relationships of Catechol O-Methyltransferase Inhibitors. *J. Comput.-Aided Mol. Design* **1992**, *6*, 253−272.
(21) Lautala, P.; Ulmanen, I.; Taskinen, J. Molecular mechanisms controlling the rate and specificity of catechol O-methylation by human soluble catechol O-methyltransferase. *Mol. Pharmacol.* **2001**, *59*, 393−402.
(22) Wikberg, T.; Vuorela, A. Metabolite profiles of two [14C]-labeled catechol O-methyltransferase inhibitors, nitecapone and entacapone, in rat and mouse urine and rat bile. *Eur. J. Drug Metabolism Pharmacokinetics* **1994**, *19*, 125−135.
(23) Jorga, K.; Fotteler, B.; Heizmann, P.; Gasser, R. Metabolism and excretion of tolcapone, a novel inhibitor of catechol-O-methyltransferase. *Br. J. Clin. Pharmacol.* **1999**, *48*, 513−520.
(24) Creveling, C. R.; Morris, N.; Shimizu, H.; Ong, H. H.; Daly, J. Catechol O-methyltransferase. IV. Factors affecting m- and *p*-methylation of substituted catechols. *Mol. Pharmacol.* **1972**, *8*, 398−409.
(25) Hou, T. J.; Xu, X. J. Three-dimensional quantitative structure−activity relationship analyses of a series of cinnamamides. *Chemom. Intell. Lab. Syst.* **2001**, *56*, 123−132.
(26) Huang, C. K.; Gao, Y.; Liu, Z. M.; Liu, Y.; Lai, L. H. Comparative molecular field analysis of pyrrolidine inhibitors for human cytosolic phospholipase A2. *Acta Phys.-Chim. Sin.* **2003**, *19*, 79−81.
(27) Liu, H.; Huang, X. Q.; Shen, J. H.; Luo, X. M.; Li, M. H.; Xiong, B.; Chen, G.; Shen, J. K.; Yang, Y. M.; Jiang, H. L.; Chen, K. X. Inhibitory mode of 1,5-diarylpyrazole derivatives against cyclooxygenase-2 and cyclooxygenase-1: Molecular docking and 3D QSAR analyses. *J. Med. Chem.* **2002**, *45*, 4816−4827.
(28) Huang, X. Q.; Xu, L. S.; Luo, X. M.; Fan, K. N.; Ji, R. Y.; Pei, G.; Chen, K. X.; Jiang, H. L. Elucidating the inhibiting mode of AHPBA derivatives against HIV-1 protease and building predictive 3D-QSAR models. *J. Med. Chem.* **2002**, *45*, 333−343.
(29) Guo, Z. R.; Yi, X.; Wang, M. M.; Chu, F. M. Molecular modeling and QSAR studies on the interaction mechanism of retinoids binding to RXR. *Acta Chim. Sin.* **2001**, *59*, 1925−1931.
(30) Jalaie, M.; Erickson, J. A. Homology model directed alignment selection for comparative molecular field analysis: Application to photosystem II inhibitors. *J. Comput.-Aided Mol. Design* **2000**, *14*, 181−197.
(31) Bernard, P.; Kireev, D. B.; Chretien, J. R.; Fortier, P. L.; Coppet, L. Automated docking of 82 N-benzylpiperidine derivatives to mouse acetylcholinesterase and comparative molecular field analysis with 'natural' alignment. *J. Comput.-Aided Mol. Design* **1999**, *13*, 355−371.

CI034189K